Natural Resources Canada | Ressources naturelles Canada

Pore structure versus texture relationship of sediment samples from a research well in the Beaufort-Mackenzie Basin, Northwest Territories

S. Connell-Madore and T.J. Katsube

Geological Survey of Canada

Current Research 2008-19

2008

Canada

Geological Survey of Canada
Current Research 2008-19

Pore structure versus texture relationship of sediment samples from a research well in the Beaufort-Mackenzie Basin, Northwest Territories

S. Connell-Madore and T.J. Katsube

2008

ISSN 1701-4387
Catalogue No. M44-2008/19E-PDF
ISBN 978-1-100-11064-6

A copy of this publication is also available for reference in depository libraries across Canada through access to the Depository Services Program's Web site at http://dsp-psd.pwgsc.gc.ca

A free digital download of this publication is available from GeoPub:
http://geopub.nrcan.gc.ca/index_e.php

Toll-free (Canada and U.S.A.): 1-888-252-4301

Recommended citation

Connell-Madore, S. and Katsube, T.J., 2008: Pore structure versus texture relationship of sediment samples from a research well in the Beaufort-Mackenzie Basin, Northwest Territories; Geological Survey of Canada, Current Research 2008-19, 8 p.

Critical reviewers
M. Hinton

Authors
S. Connell-Madore *(sconnell@nrcan.gc.ca)*
T.J. Katsube *(jkatsube@nrcan.gc.ca)*
Geological Survey of Canada
601 Booth Street
Ottawa, Ontario K1A 0E8

Correction date:

Pore structure versus texture relationship of sediment samples from a research well in the Beaufort-Mackenzie Basin, Northwest Territories

S. Connell-Madore and T.J. Katsube

Connell-Madore, S. and Katsube, T.J., 2008. Pore structure versus texture relationship of sediment samples from a research well in the Beaufort-Mackenzie Basin, Northwest Territories; Geological Survey of Canada, Current Research 2008-19, 8 p.

Abstract: Pore structure versus sediment texture relationship has been examined for 28 sedimentary rock samples (908–1090 m depth) from a research well in the Northwest Territories to provide information required to analyze the effect of texture on hydrocarbon-seal quality. Pore structure is represented by nanopore (ϕ_{np}: 2.5–25 nm), intermediate-pore (ϕ_{ip}: 0.025–10 µm), and micropore (ϕ_{mp}: 10–250 µm) porosities, in addition to storage-pore (ϕ_s) and connecting-pore (ϕ_C) porosities. Sediment texture is represented by clay, silt, and sand contents.

Results show that micropore porosity increases with increased sand and decreases with increased clay and silt contents. These results indicate that clay and silt are pore-filling material, a conclusion consistent with previous work. The intermediate-pore porosity increases with increased silt and clay, but decreases with increased sand content. The nanopore porosity lacks any distinct relationships with grain size. For increasing micropore porosity values, connecting-pore porosity generally decreases and for micropore porosity greater than 3% values, storage-pore porosity increases.

Résumé : Un examen de la relation entre la structure poreuse et la texture sédimentaire a été réalisé sur 28 échantillons de roches sédimentaires, prélevés entre 908 et 1 090 m de profondeur dans un puits de recherche dans les Territoires du Nord-Ouest, dans le but de fournir l'information nécessaire à l'analyse des effets de la texture sur la qualité d'étanchéité pour les hydrocarbures. La structure poreuse est exprimée suivant les porosités de nanopores (ϕ_{np} : 2,5 –25 nm), de pores de taille intermédiaire (ϕ_{ip} : 0,025–10 µm) et de micropores (ϕ_{mp} : 10–250 µm), ainsi que suivant les porosités de stockage (ϕ_s) et de communication (ϕ_C). La texture sédimentaire est fondée sur la teneur en argile, en silt et en sable.

Les résultats montrent que les valeurs de la porosité de micropores augmentent lorsque la proportion de sable augmente, alors qu'elles diminuent lorsque les proportions d'argile et de silt augmentent. Ces résultats indiquent que l'argile et le silt sont des matériaux de remplissage des pores, une conclusion en accord avec celle de travaux antérieurs. Les valeurs de la porosité de pores de taille intermédiaire augmentent lorsque les proportions de silt et d'argile augmentent, mais diminuent lorsque la proportion de sable augmente. Les valeurs de la porosité de nanopores ne présentent aucun lien distinct avec la granulométrie. Lorsque les valeurs de la porosité de micropores augmentent, généralement la porosité de stockage diminue et, pour des valeurs de la porosité de micropores supérieures à 3 %, la porosité de stockage augmente.

INTRODUCTION

The relationship between pore structure and sediment texture has been examined for 28 sedimentary rock samples collected from a depth range of 908.05–1089.89 m in the Mallik 5L-38 research well, Northwest Territories (Katsube et al., 2005). This well was drilled as part of the JAPEX/JNOC/GSC gas hydrate project of 2003 (Dallimore et al., 2005). The main formations at these depths consist of clayey silt, fine sand, silty sand, and medium-sand mudstone (Collett et al., 2005). The purpose of this study was to examine the effect of sediment texture on pore structure. This is part of a project to study the effect of sediment texture on hydrocarbon-seal quality (Katsube et al., 2006; Katsube and Connell-Madore, 2008) of sedimentary rocks.

It is well known that an increased clay content decreases the fluid permeability and increases the seal quality (e.g. Yang and Aplin, 2007) of sedimentary rocks. A recent study, however, has shown that an increase of both clay and silt contents contribute to decreased gas permeability (k_G) and increased seal quality (Katsube and Connell-Madore, 2008).

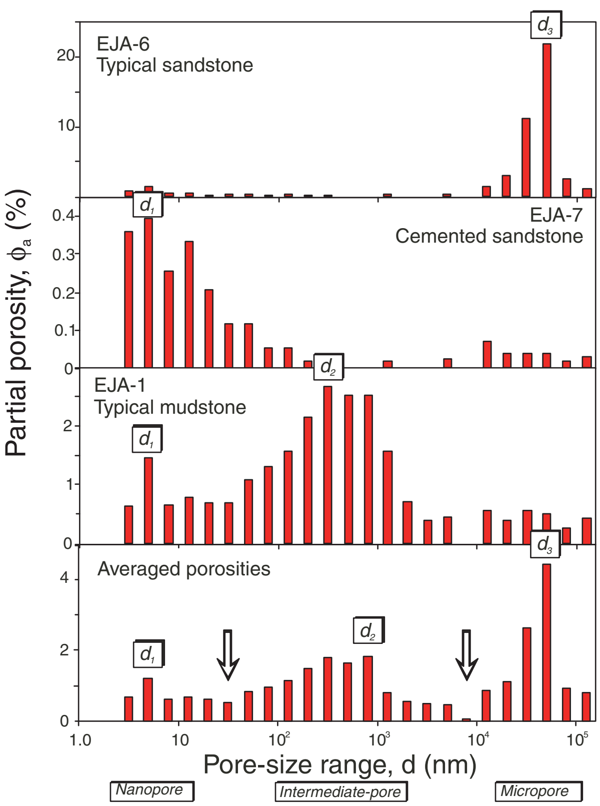

Figure 1. Representative pore-size distributions and their modes (d_1, d_2, and d_3)(*modified from* Katsube et al., 1999) for **a)** unconsolidated sandstone, **b)** cemented sandstone, **c)** mudstone, and **d)** average pore-size distribution of the 28 samples used in this study, from the JAPEX/JNOC/GSC Mallik 2L-38 research well. The vertical arrows in Figure 1d indicate the boundaries between the nanopore porosities (ϕ_{np}: 2.5–25 nm), intermediate-pore porosities (ϕ_{ip}: 25 nm to 10 µm), and the micropore porosities (ϕ_{mp}: 10–250 µm).

In addition, that study shows that certain combinations of some larger grains (e.g. fine and medium sand) can also contribute to lower k_G and increased seal quality; however, currently there is only limited knowledge on the effect of sediment texture on pore structure. Pore structure, in this case, is represented by the nanopore porosity (ϕ_{np}), intermediate-pore porosity (ϕ_{ip}), micropore porosity (ϕ_{mp}), storage-pore porosity (ϕ_S), and connecting-pore porosity (ϕ_C). The sediment texture, in this case, is represented by the grain-size distributions of these sedimentary rock samples (Connell-Madore and Katsube, 2007a). The ϕ_{np}, ϕ_{ip}, and ϕ_{mp} are porosities for the pore-size (d) ranges of 2.5–25 nm, 25 nm to 10 µm, and 10–250 µm. This pore-size classification is based on a previous study (Fig. 1, Katsube et al., 1999; Fig. 1), using similar samples from a different well, showing that ϕ_{ip} and ϕ_{mp} generally increase with increased silt and sand contents (Fig. 2), respectively. The relationship between ϕ_{np} and clay content was considered constant in that study. The ϕ_S and ϕ_C are the porosities of the pores that mainly contribute to storing and transporting fluids in rocks and their models are shown in Figure 3 (Katsube and Williamson, 1998). Although it is reasonable for them to be related to the grain sizes, that relationship could be very complex if there is morphology variation related to the different grain sizes, such as clay and sand. Therefore, in this study, the possibility of an indirect relationship existing with grain sizes is considered by examining their relationship to the other three porosities (ϕ_{np}, ϕ_{ip}, and ϕ_{mp}). In this paper, the authors first describe the method of investigation, followed by the analytical results, and then the discussion and conclusions of the analytical results.

METHOD OF INVESTIGATION AND RESULTS

The pore-structure data for these 28 samples used in this study have been presented in previous publications (Katsube et al., 2005; Connell-Madore and Katsube, 2007b) and are listed in Table 1. These data were obtained from mercury-injection porosimetry measurements (Washburn, 1921; Rootare, 1970) performed by the AGAT Laboratories (Calgary, Alberta). The storage-porosity (ϕ_S) and connecting-porosity (ϕ_C) (Fig. 3) data, in the table, were also produced using mercury-injection porosimetry techniques listed in previous publications (e.g. Katsube et al., 1997, 1999; Bowers and Katsube, 2002). The nanopore porosity (ϕ_{np}), intermediate-pore porosity (ϕ_{ip}), and micropore porosities (ϕ_{mp}) in the same table represent porosity values for pore-size (d) ranges between 2.5–25 nm, 25 nm to 10 µm, and 10–250 µm, as previously indicated. The values for these pore-size boundaries are based on the average pore-size distribution of a set of sedimentary rock samples shown in Figure 1d (Katsube et al., 1999). These pore-size boundaries have also been used in subsequent studies for sedimentary rocks (Katsube and Connell-Madore, 2008). The relationship between these porosities and the effective porosity (ϕ_E), which is the total interconnected porosity, is as follows:

$$\phi_E = \phi_S + \phi_C, \qquad (1)$$

$$\phi_E = \phi_{np} + \phi_{ip} + \phi_{mp}. \qquad (2)$$

The grain-size distribution data obtained from a previous publication (Connell-Madore and Katsube, 2007a) are listed in Table 2. The grain-size distribution data was also produced by AGAT Laboratories (Calgary, Alberta). The grain-size classification system for clay (<3.9 µm), silt (3.9–62.5 µm), and sand (>62.5 µm) is based on the Wentworth grain-size classification system (Folk, 1968).

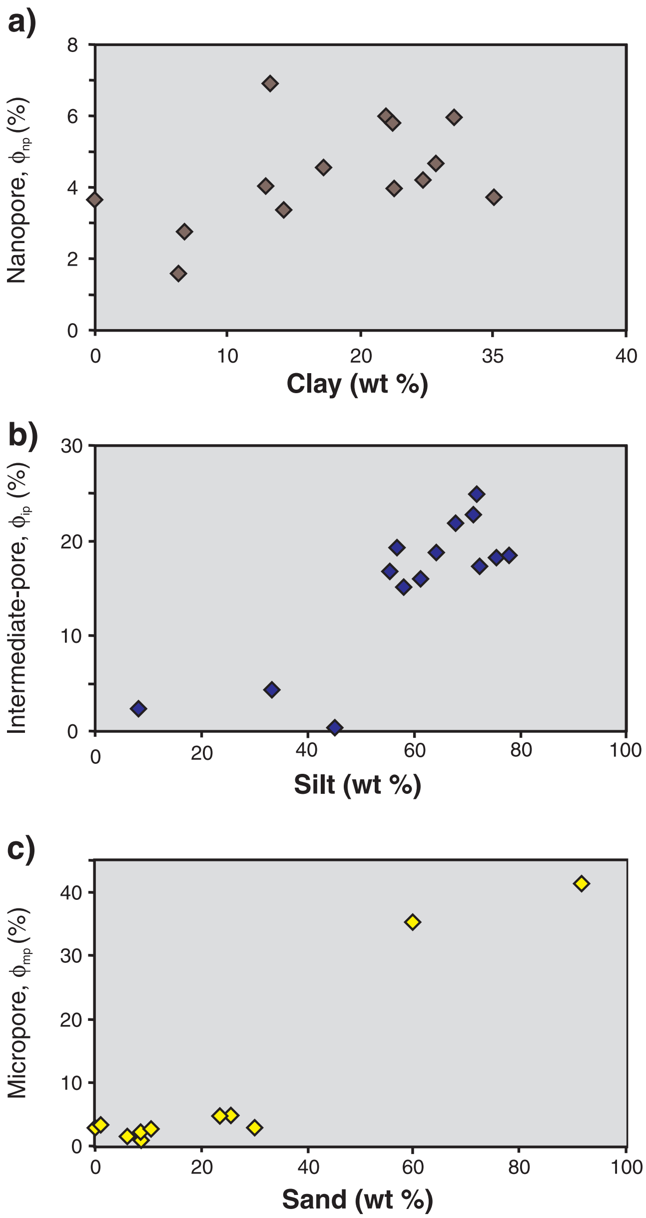

Figure 2. Relationships between pore-structure porosities and total clay, silt, and sand contents of the consolidated mudstone seen in a previous publication (Katsube et al., 1999): **a)** for nanopore porosity (ϕ_{np}), **b)** for intermediate-pore porosity (ϕ_{ip}), and **c)** for micropore porosity (ϕ_{mp}).

DATA ANALYSIS

The micropore porosities (ϕ_{mp}) plotted against the three grain-size components (clay, silt, sand) for this study are shown in Figure 4. The ϕ_{mp} shows a general decrease for both increased clay (Fig. 4a) and silt (Fig. 4b) contents. On the other hand, although there is a considerable scatter, ϕ_{mp} shows a general increase with increased sand content (Fig. 4c), which is similar to that of the previous study shown in Figure 4c. The intermediate-pore porosities (ϕ_{ip}) plotted against the three grain-size components (clay, silt, sand) for this study are shown in Figure 5. The ϕ_{ip} shows a general increase for both increased clay (Fig. 5a) and silt (Fig. 5b) contents, but a general decrease with increased sand content (Fig. 5c). This ϕ_{ip} versus silt relationship in Figure 5b is also similar to that of the previous study in Figure 2b. The nanopore porosities (ϕ_{np}) plotted against the three grain-size components (clay, silt, sand) for this study are shown in Figure 6. The ϕ_{np} does not show any general increasing or decreasing trends with the increased contents of the three grain-size components and can be considered independent of grain size, similar to the ϕ_{np} versus clay relationship of Katsube et al. (1999) in Figure 2a.

Storage porosity (ϕ_s) and connecting porosity (ϕ_C) are plotted against ϕ_{np}, ϕ_{ip}, and ϕ_{mp} in Figure 7. There is no distinct relationship that can be observed between these two porosities (ϕ_S, ϕ_C) with increased ϕ_{np} or ϕ_{ip} values in Figures 7a or 7b. In Figure 7c, although the data are scattered, it is possible to consider a general decreasing trend for ϕ_c with increased ϕ_{mp}. For the ϕ_s versus ϕ_{mp} relationship in Figure 7c, it seems that there is a break at the ϕ_{mp} value of 3%. It appears that for ϕ_{mp} less than 3%, the ϕ_s versus ϕ_{mp}

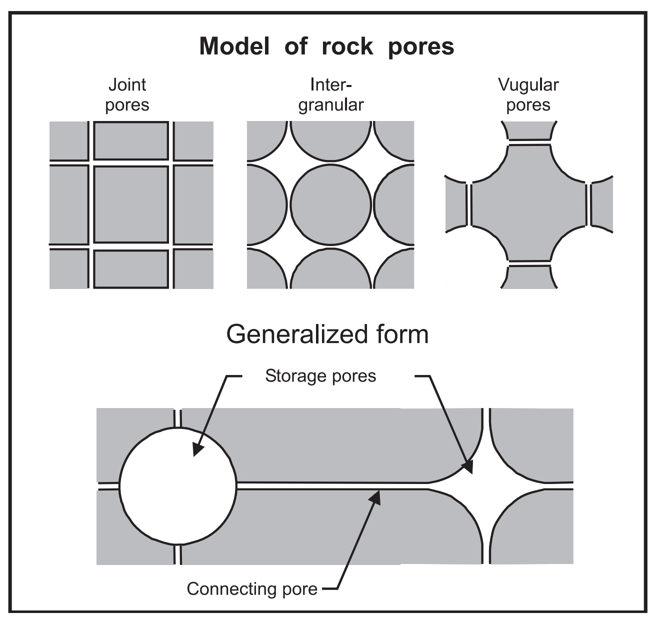

Figure 3. Storage (ϕ_S) and connecting-pore (ϕ_C) model (Katsube and Williamson, 1998).

Table 1. Pore-structure (Katsube et al., 2005) data represented by porosities (%) and main modes (μm) of the pore-size distributions for the 28 sediment samples used in this study.

Sample number	Depth, h (m)	ϕ_s (%)	ϕ_c (%)	ϕ_{np} (%)	ϕ_{ip} (%)	ϕ_{mp} (%)	d_G (μm)	d_M (nm)
P2EJA-11	908.05	40.91	0.61	0.05	9.52	31.94	234.1	13.28
P2EJA-26	910.61	4.18	12.90	0.06	0.23	16.82	373.1	8.75
P2EJA-16	916.19	1.93	9.12	2.38	0.32	8.35	194.2	5.36
P2EJA-17	918.95	46.48	0.93	0.10	0.28	47.00	194.2	30.75
P2EJA-21	920.81	32.07	2.39	0.00	0.13	33.34	176.8	25.01
P2EJA-27	925.09	32.89	3.87	1.94	13.37	21.33	161.2	5.28
P2EJA-7	927.35	2.31	6.96	0.47	1.66	7.15	339.8	5.21
P2EJA-25	933.58	9.67	5.60	0.36	13.21	2.18	146.8	3.67
P2EJA-4	937.47	12.69	3.47	0.11	13.40	2.66	18.9	3.06
P2EJA-13	939.88	10.77	6.89	0.39	16.10	1.17	20.7	3.69
P2EJA-19	953.47	15.69	10.39	0.04	3.93	22.14	146.8	6.16
P2EJA-2	955.69	24.37	3.93	3.38	3.62	21.31	493.6	6.21
P2EJA-20	972.05	14.13	5.64	1.24	15.50	3.03	18.9	3.28
P2EJA-14	973.08	26.63	2.95	0.60	5.78	23.20	339.8	6.17
P2EJA-22	975.67	40.82	0.67	0.31	4.29	36.89	282.1	10.68
P2EJA-5	980.65	0.43	7.28	0.34	0.87	6.52	309.6	6.17
P2EJA-10	982.59	10.93	7.63	0.52	16.91	1.16	20.7	3.35
P2EJA-28	987.53	35.76	3.40	1.28	12.72	25.16	194.2	8.37
P2EJA-1	989.73	2.42	12.60	1.83	0.27	12.82	282.1	7.40
P2EJA-8	1004.93	8.46	8.90	0.90	14.68	1.78	8.9, 161.2	5.25
P2EJA-24	1022.42	3.00	10.64	1.31	0.56	11.78	282.1	4.48
P2EJA-15	1028.78	12.13	9.40	0.29	20.00	1.28	18.9	8.58
P2EJA-9	1042.12	13.39	7.53	0.58	18.35	2.01	8.1	5.93
P2EJA-18	1063.47	13.24	7.59	0.63	18.86	1.36	18.9	4.33
P2EJA-12	1072.75	11.67	5.21	0.54	1.08	15.28	121.8	4.57
P2EJA-6	1076.63	8.90	1.64	0.79	1.45	8.27	256.8	3.91
P2EJA-3	1083.45	12.92	6.24	0.10	16.84	2.20	18.9	4.31
P2EJA-23	1089.89	12.55	11.35	0.05	6.88	16.82	282.1	8.78

h = Depth.
ϕ_S = Storage porosity.
ϕ_C = Connecting porosity.
ϕ_{np} = Nanopore porosity (2.5–25 nm).
ϕ_{ip} = Intermediate-pore porosity (25 nm to 10 μm).
ϕ_{mp} = Micropore porosity (10–250 μm).
d_G = Main mode of the grain-size distribution (μm).
d_M = Main mode of the pore-size distribution (nm).

relationship is more or less constant. For the ϕ_{mp} values greater than 3%, ϕ_s appears to show a strong increasing trend with increased ϕ_{mp} values.

DISCUSSION AND CONCLUSIONS

Figure 4, which shows the micropore porosities (ϕ_{mp}) plotted against the three grain-size components (clay, silt, sand), is very interesting. Although the data are very scattered, it is possible to consider ϕ_{mp} showing a general increase with increased sand content (Fig. 4c). This trend is expected, since the sand grains generally form the framework grains and ϕ_{mp} is expected to represent the intergranular pore spaces between these grains. Again although the data are scattered, ϕ_{mp} shows a general decrease for both increased clay (Fig. 4a) and silt (Fig. 4b) contents. These are also generally expected trends, since both of these grain sizes are expected to fill and reduce the pore spaces between the framework grains. These trends are consistent with results of a previous study (Katsube and Connell-Madore, 2008), which showed the gas-permeability (k_G) values increasing with increased sand content, and k_G decreasing with increased clay and silt contents. In Figure 5, the intermediate-pore porosity (ϕ_{ip}) increase with increased silt content (Fig. 5b) was expected since ϕ_{ip} was associated with a silt increase in a previous study (Katsube et al., 1999) as shown in Figure 2b; however, the general increase of ϕ_{ip} with increased clay content (Fig. 5a) and general decrease of ϕ_{ip} with increased sand content (Fig. 5c) were not expected and requires further analysis for an explanation. In Figure 6 the nanopore porosity (ϕ_{np}) lacks any distinct increasing or decreasing trends to be seen with increased contents of the three grain-size components (clay, silt, sand). That trend for ϕ_{np} versus clay (Fig. 6a) is consistent with a previous study (Katsube et al., 1999), as shown in Figure 2a; however, the reason for these trends needs further analysis for an explanation. In Figure 7, the storage porosity (ϕ_s) and connecting porosity (ϕ_C) are plotted against ϕ_{np}, ϕ_{ip}, and ϕ_{mp}. Both ϕ_s and

Table 2. Grain-size data (volume, per cent) for the 28 sediment samples (Connell-Madore and Katsube, 2007a) used in this study.

Sample number	Depth, h (m)	Clay (<3.9 µm) (%)	Silt (3.9–62.5 µm) (%)	Sand (>62.5 µm) (%)
P2EJA-1	989.73	4.61	13.80	81.59
P2EJA-2	955.69	1.37	3.88	94.72
P2EJA-3	1083.45	20.70	62.70	16.61
P2EJA-4	937.47	18.24	46.87	34.93
P2EJA-5	980.65	4.66	11.79	83.53
P2EJA-6	1076.63	4.81	14.83	80.37
P2EJA-7	927.35	3.68	11.48	84.85
P2EJA-8	1004.93	19.58	51.70	28.73
P2EJA-9	1042.12	30.85	68.75	0.41
P2EJA-10	982.59	26.79	64.02	9.21
P2EJA-11	908.05	7.69	22.16	70.14
P2EJA-12	1072.75	15.51	38.16	46.33
P2EJA-13	939.88	21.41	73.96	4.63
P2EJA-14	973.08	7.03	18.51	74.44
P2EJA-15	1028.78	25.30	71.20	3.51
P2EJA-16	916.19	1.46	4.70	93.87
P2EJA-17	918.95	2.09	5.37	92.52
P2EJA-18	1063.47	25.81	47.35	26.86
P2EJA-19	953.47	6.21	24.50	69.28
P2EJA-20	972.05	23.95	60.89	15.18
P2EJA-21	920.81	2.62	7.65	89.68
P2EJA-22	975.67	5.93	14.15	79.92
P2EJA-23	1089.89	6.02	20.28	73.70
P2EJA-24	1022.42	4.63	16.36	79.08
P2EJA-25	933.58	9.88	36.50	53.65
P2EJA-26	910.61	2.78	7.75	89.47
P2EJA-27	925.09	4.14	13.14	82.76
P2EJA-28	987.53	13.53	32.74	53.78

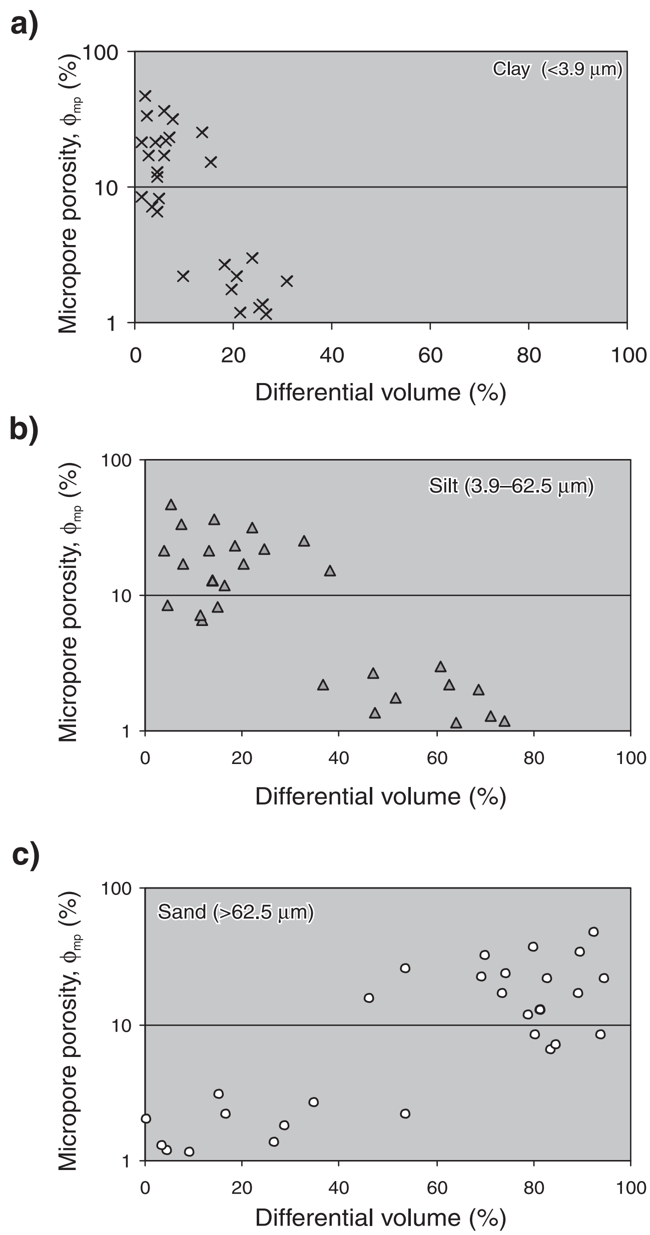

Figure 4. Relationships between the micropore porosity (ϕ_{mp}) and **a)** clay (<3.9 µm), **b)** silt (3.9–62.5 µm), and **c)** sand (>62.5 µm) contents.

ϕ_C lack any distinct relationships with ϕ_{np} and ϕ_{ip} in Figures 7a and 7b. In Figure 7c, however, although scattered, ϕ_C can be considered to show a general decrease with increased ϕ_{mp} values. In the same figure, the ϕ_s versus ϕ_{mp} relationship is more or less constant for ϕ_{mp} less than 3%, and ϕ_s appears to show a strong increasing trend with increased ϕ_{mp} values for ϕ_{mp} greater than 3%. These trends are interesting and suggest further analysis should be carried out.

As a general conclusion, this study has shown that sediment texture does have an effect on pore structure. It shows that not only clay, as stated in the literature (e.g. Yang and Aplin, 2007), but silt and certain combinations of larger grains can also have an effect on reducing pore spaces and improving seal quality. It also indicates that further study and analysis is required to fully understand the effect of texture on seal quality.

ACKNOWLEDGMENTS

The authors are grateful to M. Hinton (GSC Ottawa) for critically reviewing this paper and for his very constructive and useful comments. Both the mercury-injection porosimetry and grain-size distribution measurements were performed at AGAT Laboratories (Calgary, Alberta). The authors would also like to acknowledge S. Dallimore (GSC Pacific) for supplying the samples used in this study.

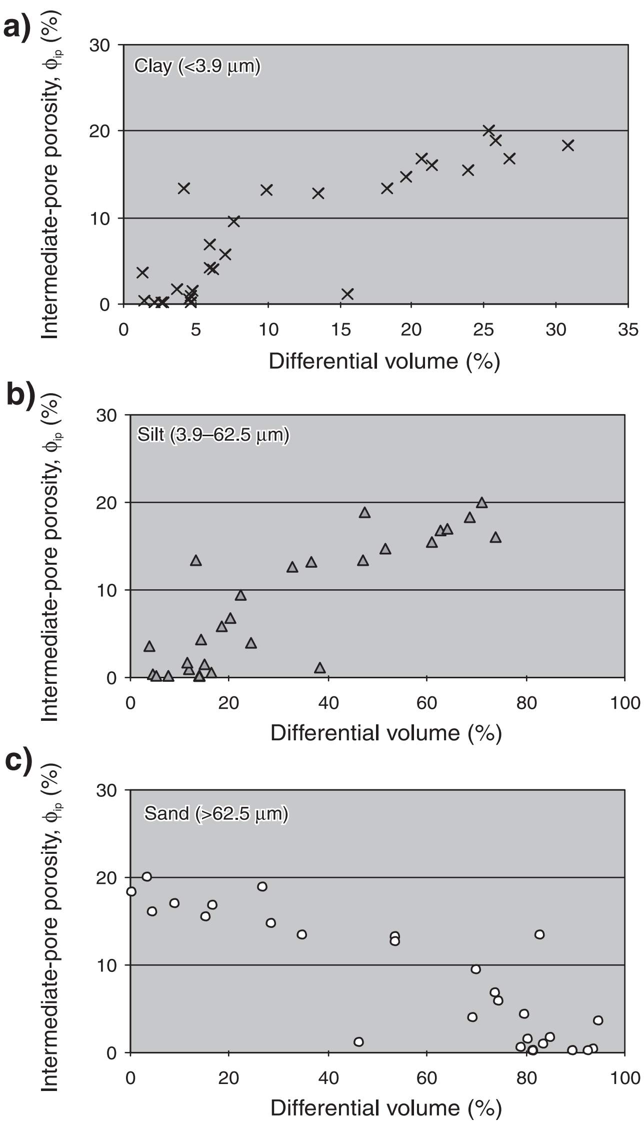

Figure 5. Relationships between the intermediate-pore porosity (ϕ_{ip}) and **a)** clay (<3.9 µm), **b)** silt (3.9–62.5 µm), and **c)** sand (>62.5 µm) contents. There is no data for the clay content above 35% (Fig. 5a).

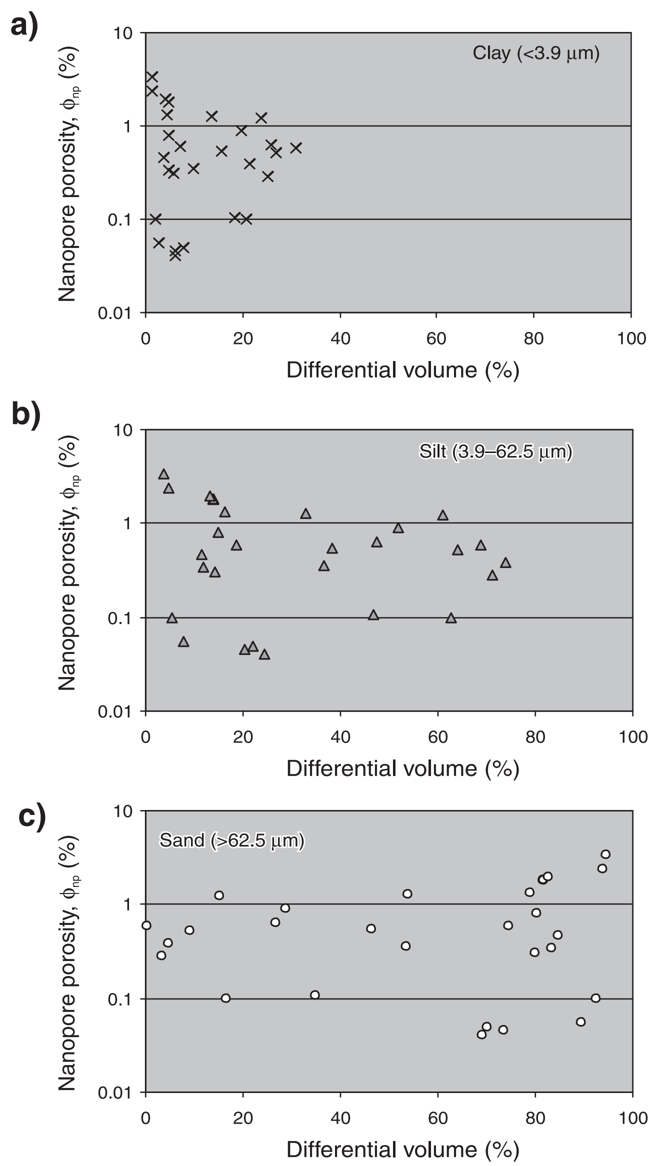

Figure 6. Relationships between the nanopore porosity (ϕ_{np}) and **a)** clay (<3.9 µm), **b)** silt (3.9–62.5 µm), and **c)** sand (>62.5 µm) contents.

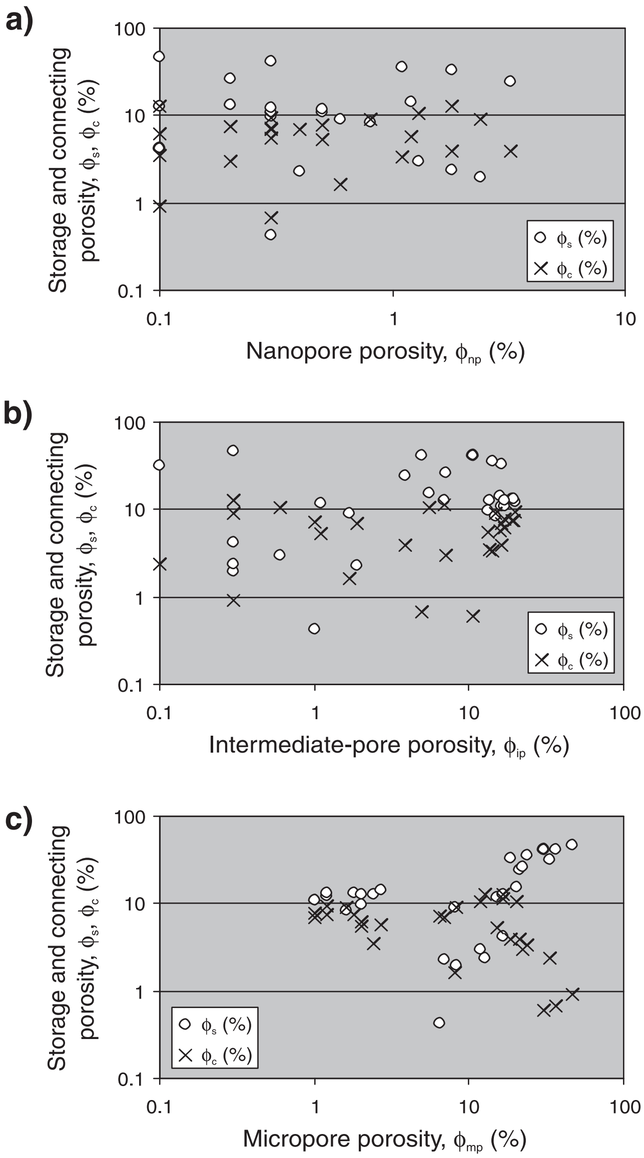

Figure 7. Relationships between the storage (ϕ_S) and connecting-pore porosities (ϕ_C) and the **a)** nanopore porosity (ϕ_{np}), **b)** intermediate-pore porosity (ϕ_{ip}), and **c)** micropore porosities (ϕ_{mp}).

REFERENCES

Bowers, G.L. and Katsube, T.J., 2002. The role of shale pore-structure on the sensitivity of wireline logs to overpressure; *in* Pressure Regimes in Sedimentary Basins and their Prediction, (ed.) A.R. Huffman and G.L. Bowers; American Association of Petroleum Geologists, Memoir 76, p. 43–60.

Collett, T.S., Lewis, R.E., and Dallimore, S.R., 2005. JAPEX/JNOC/GSC et al. Mallik 5L-38 gas hydrate production research well downhole well-log and core montages; *in* Scientific Results from the Mallik 2002 Gas Hydrate Production Research Well Program, Mackenzie Delta, Northwest Territories, Canada, (ed.) S.R. Dallimore and T.S. Collett; Geological Survey of Canada, Bulletin 585, 23 p.

Connell-Madore, S. and Katsube, T.J., 2007a. Grain-size distribution and gas permeability of sediment samples from the JPEX/JNOC/GSC et al. Mallik 5L-38 gas hydrate production research well, Northwest Territories; Geological Survey of Canada, Current Research 2007-B6, 13 p.

Connell-Madore, S. and Katsube, T.J., 2007b. Pore-size distribution of samples from the Mallik 5L-38 well, Northwest Territories; Geological Survey of Canada, Current Research 2007-B2, 11 p.

Dallimore, S.R., Medioli, B.E., Laframboise, R.R., and Giroux, D. (comp.), 2005. Mallik 2002 Gas Hydrate Production Research Well Program, Mackenzie Delta, Northwest Territories: well data and interactive data viewer; Appendix A *in* Scientific Results from the Mallik 2002 Gas Hydrate Production Research Well Program, Mackenzie Delta, Northwest Territories, Canada, (ed.) S.R. Dallimore and T.S. Collett; Geological Survey of Canada, Bulletin 585 (DVD).

Folk, R., 1968. Petrology of Sedimentary Rocks; Hemphill's Book Store, Austin, Texas, 170 p.

Katsube, T.J. and Connell-Madore, S., 2008. Gas permeability versus texture relationship of sediment samples from a research well in the Beaufort-Mackenzie Basin, Northwest Territories; Geological Survey of Canada, Current Research 2008-4, 10 p.

Katsube, T.J. and Williamson, M.A., 1998. Shale petrophysical characteristics: permeability history of subsiding shales; *in* Shales and Mudstones, Volume II: Petrography, Petrophysics, Geochemistry and Economic Geology, (ed.) J. Schiber, W. Zimmerle, and P.S. Sethi; Schweizerbart'sche Verlagsbuchhandlung, Stuttgart, Germany, p. 69–91.

Katsube, T.J., Dallimore, S.R., Jonnasson, I.R., Connell-Madore, S., Medioli, B.E., Uchida, T., Wright, J.F., and Scromeda, N., 2005. Petrophysical characteristics of gas-hydrate-bearing and gas-hydrate-free formations in the JAPEX/JNOC/GSC et al Mallik 5L-38 gas hydrate production research well; *in* Scientific Results from the Mallik 2002 Gas Hydrate Production Research Well Program, Mackenzie Delta, Northwest Territories, Canada, (ed.) S.R. Dallimore and T.S. Collett; Geological Survey of Canada, Bulletin 585, 14 p.

Katsube, T.J., Dallimore, S.R., Uchida, T., Jenner, K.A., Collett, T.S., and Connell, S., 1999. Petrophysical environment of sediments hosting gas-hydrate, JAPEX/JNOC/GSC Mallik 2L-38 gas hydrate research well; *in* Scientific Results from JAPEX/JNOC/GSC Mallik 2L-38 Gas Hydrate Research Well, Mackenzie Delta, Northwest Territories, Canada, (ed.) S.R. Dallimore, T. Uchida, and T.S. Collett; Geological Survey of Canada, Bulletin 544, p. 109−124.

Katsube, T.J., Dorsch, J., and Connell, S., 1997. Pore surface area characteristics of the Nolichucky Shale within the Oak Ridge Reservation (Tennessee, USA): implication for fluid expulsion efficiency; *in* Current Research 1997-E; Geological Survey of Canada, p. 117−124.

Katsube, T.J., Issler, D.R., and Connell-Madore, S., 2006. Storage and connecting pore structure of mudstone-shale and its effect on seal quality: tight shales that may leak; *in* Abstract Volume of AAPG International Conference and Exhibition, November 5−8, 2006, Perth, Australia, p. 60.

Rootare, H.M., 1970. A review of mercury porosimetry; Perspectives of Powder Metallurgy, v. 5, p. 225–252.

Washburn, E.W., 1921. Note on a method of determining the distribution of pore sizes in a porous material; Proceedings of the National Academy of Sciences of the United States of America, v. 7, p. 115–116. doi:10.1073/pnas.7.4.115 PubMed

Yang, Y. and Aplin, A.C., 2007. Permeability and petrophysical properties of 30 natural mudstones; Journal of Geophysical Research, v. 112, no. B03206, 18 p.

Geological Survey of Canada Project Y62.